OXFORD UNIVERSITY PRESS | Human Molecular Genetics

Antisense targeting of 3'end elements involved in DUX4 mRNA processing is an efficient therapeutic strategy for Facioscapulohumeral Dystrophy: a new gene silencing approach.

Journal:	*Human Molecular Genetics*
Manuscript ID	HMG-2015-D-01434.R1
Manuscript Type:	2 General Article - UK Office
Date Submitted by the Author:	14-Jan-2016
Complete List of Authors:	Marsollier, Anne-Charlotte; Pierre and Marie Curie University, UMRS974, INSERM U974, CNRS UMR7215, Myology Institute Ciszewski, Lukasz; Royal Holloway University of London, Centre of Biomedical Sciences, School of Biological Sciences mariot, virginie; Université Paris 6, INSERM U974, UMR 7215 CNRS, Institut de Myologie, UM 76 Université Pierre et Marie Curie Popplewell, Linda; Royal Holloway - University of London, School of Biological Sciences Voit, Thomas; Pierre and Marie Curie University, UMRS974, INSERM U974, CNRS UMR7215, Myology Institute Dickson, George; Molecular Cell Biology, Royal Holloway College-University of London Dumonceaux, Julie; Pierre and Marie Curie University, UMRS974, INSERM U974, CNRS UMR7215, Myology Institute
Key Words:	FSHD, muscle, gene silencing, DUX4, polyadenylation

Antisense targeting of 3'end elements involved in *DUX4* mRNA processing is an efficient therapeutic strategy for Facioscapulohumeral Dystrophy: a new gene silencing approach.

Anne-Charlotte Marsollier[1], Lukasz Ciszewski[2#], Virginie Mariot[1#], Linda Popplewell[2], Thomas Voit[1,§], George Dickson[2], Julie Dumonceaux[1*]

[1]Sorbonne Universités UPMC Univ Paris 06, Inserm, CNRS, Centre de Recherche en Myologie (CRM), GH Pitié Salpêtrière, 47 bld de l'hôpital, Paris 13, France

[2]Centre of Biomedical Sciences, School of Biological Sciences, Royal Holloway University of London, Surrey, TW20 0EX UK

[§]Present Address: NIHR Biomedical Research Centre, Institute of Child Health, University College London, 30 Guilford Street, London WC1N1EH, UK

# equal contribution

*Corresponding author: Julie Dumonceaux

Corresponding author's address: Sorbonne Universités UPMC Univ Paris 06, Inserm, CNRS, Centre de Recherche en Myologie (CRM), GH Pitié Salpêtrière, 47 bld de l'hôpital, Paris 13, France

Corresponding author's phone and fax: +33 1 42 16 57 16 and + 33 1 42 16 57 00

Corresponding author's e-mail address: julie.dumonceaux@upmc.fr

ABSTRACT

Defects in mRNA 3' end formation have been described to alter transcription termination, transport of the mRNA from the nucleus to the cytoplasm, stability of the mRNA and translation efficiency. Therefore, inhibition of polyadenylation may lead to gene silencing. Here, we choose Facioscapulohumeral Dystrophy (FSHD) as a model to determine whether or not targeting key 3'end elements involved in mRNA processing using antisense oligonucleotide drugs can be used as a strategy for gene silencing within a potentially therapeutic context. FSHD is a gain-of-function disease characterized by the aberrant expression of the DUX4 transcription factor leading to altered pathogenic deregulation of multiple genes in muscles. Here we demonstrate that targeting either the mRNA polyadenylation signal and/ or cleavage site is an efficient strategy to downregulate *DUX4* expression and to decrease the abnormally high pathological expression of genes downstream of DUX4. We conclude that targeting key functional 3'end elements involved in pre-mRNA to mRNA maturation with antisense drugs can lead to efficient gene silencing and is thus a potentially effective therapeutic strategy for at least FSHD. Moreover polyadenylation is a crucial step in the maturation of almost all eukaryotic mRNAs, and thus all mRNAs are virtually eligible for this antisense-mediated knockdown strategy.

INTRODUCTION

The cleavage and polyadenylation of the 3' end of pre-mRNAs are fundamental processing steps for the maturation of the vast majority of eukaryotic mRNAs. In human cells, these reactions are governed by more than 80 RNA-binding proteins and by regulatory cis-acting RNA sequence elements (for reviews see (1-3)). The key element dictating the cleavage is a 6 nucleotide (nt) motif called the poly(A) signal (PAS). Most of the mammalian mRNAs contain the PAS consensus AAUAAA or AUUAAA hexamer or close variants (4-6) which is recognized by the multimeric set of cleavage and polyadenylation factors. This RNA-protein interaction determines the site of cleavage which usually occurs 10-30 nt downstream of the PAS. The second important element is a U/GU-rich sequence (Downstream Sequence Element, DSE) contacted by the cleavage stimulation factor (CstF) and located 30-60 nt downstream the PAS motif (for review see (7)). In most cases, these co-transcriptional maturations are required for nuclear export and stability of mRNAs, and their efficient translation (8), and thus consequently represent attractive and interesting drug and/or genetic targets for suppression of gene expression. Indeed, the functional importance of the 3'end mRNA processing has been highlighted by the discovery of mutations in the PAS cis-element causing or contributing to human diseases including haemotologic diseases, neurogenerative diseases, or cancer (for review see (9)).

The aim of our study was to determine whether or not targeting elements involved in pre-mRNA maturation (such as PAS or DSE) using antisense oligonucleotide drugs can be a strategy for gene silencing within a potentially therapeutic context. We focused on Faciocapulohumeral Dystrophy (FSHD) which is a rare autosomal dominant neuromuscular disorder with an incidence of 1:14,000 to 1:20,000 characterized by the atrophy of specific groups of muscles (10). This pathology is caused by a loss of epigenetic marks within the D4Z4 macrosatellite located in the sub-telomeric region of chromosome 4 leading to

chromatin relaxation (11). In 95% of the FSHD patients (named FSHD1), this chromatin relaxation is associated with a contraction of the D4Z4 array (12, 13). The remaining 5% of the FSHD patients (named FSHD2) do not present a contraction of D4Z4 but the vast majority of them carry a mutation in the epigenetic modifier gene *SMCHD1* (14, 15) . This loss of epigenetic marks, when associated with a permissive chromosome 4 (ie carrying the 4qA haplotype containing the ATTAAA PAS commonly found in human (16)), leads to the aberrant transcription of a double homeobox transcription factor named DUX4 whose ORF is present in each D4Z4 repeat (17). DUX4 protein and mRNA have been robustly detected in adult and fetal FSHD1 and FSHD2 cells and biopsies whereas they can be found at very low levels in control (18-21)*DUX4* mRNA is only expressed in 1/1000 nuclei but DUX4 protein can be found in 0.5-9% of nuclei (18, 22), suggesting that although DUX4 is not transcribed in most nuclei, the resulting protein may spread further (23). DUX4 is a transcription factor and its overexpression is described to disturb several cellular pathways (23-30). Moreover, it was shown that even if DUX4 expression has not been directly linked to patient's phenotype, DUX4 may play a major role in the pathophysiology of FSHD because : (i) it has been shown that at least one D4Z4 repeat is needed for FSHD onset (31), (ii) only alleles with the 4qA type (containing the AUUAAA PAS for *DUX4* mRNA) are associated with FSHD (32, 33), (iii) contraction of the D4Z4 array on chromosome 10 which carries a mutated PAS (AUCAAA) does not lead to FSHD (16), (iv) DUX4-induced gene expression is the major molecular signature in FSHD skeletal muscles (34), and (v) DUX4 expression is the common point between FSHD1 and FSHD2 patients (16).

Several therapeutic strategies targeting DUX4 expression have been proposed in the literature: RNA interference, 2'-O-methyl antisense oligonucleotides (AO) targeting intron-exon junctions or over-expression of truncated DUX4 (27, 35-37). Here we describe a new therapeutic AO-based therapeutic approach for FSHD using phosphorodiamidate morpholino

oligomers (PMOs) targeting the key elements of 3'end processing of the *DUX4* transcript and which represent the key disease-permissive feature of the FSHD1 and 2 locus. Indeed, during the past 10 years, synthetic AOs have emerged as a promising strategy for drug therapy of genetic disorders affecting skeletal muscles such as the muscular dystrophies and motor-neuron diseases. PMOs have been mainly described to bind with high affinity the targeted pre-mRNAs and mRNAs and to form a stable hybrid that efficiently blocks access of splicing or translation machineries (so-called steric blocking AOs). PMOs can also form a structure mimicking a tRNA precursor which is recognized by RNaseP leading to mRNA cleavage (for review see (38, 39)). Numerous studies investigating the therapeutic potential of antisense technology have been already performed and several clinical trials are now in progress for muscular dystrophies (40-43).

In this article, we choose to target the 3' key elements of *DUX4* pre-mRNA, focusing on the disease-permissive PAS, the cleavage site and the U/GU-rich DSE sequence. We demonstrated *in vitro* that targeting the 3' end elements of mRNA with antisense drugs can be an efficient therapeutic strategy for a genetic disease. We observed that targeting *DUX4* 3'key elements leads to an efficient extinction of *DUX4*, may redirect the mRNA cleavage site and prevents aberrant expression of genes downstream of the DUX4 transcription factor.

RESULTS

Determination of 3'end key elements of *DUX4* mRNA and PMO design

For muscle tissue, one PAS (AUUAAA) has been described for *DUX4* mRNA, located 766 bp downstream of the stop codon in genomic DNA (16). Because the *DUX4* gene gives rise to two *DUX4-FL* isoforms (*DUX4-FL1* with spliced intron 1 and *DUX4-FL2* with non-spliced intron 1), the cleavage site of *DUX4* was precisely determined by RT-3'RACE-PCR using primers allowing the detection of each isoform. Total RNAs were extracted from FSHD

myotubes at day 4 of differentiation when *DUX4* expression is the highest (21). The sequences of the PCR products revealed the presence of 3 different cleavage sites located 16 to 22 bp after the PAS for both *DUX4-FL1* and -*FL2 DUX4* isoforms (Fig. 1A-B). However, these cleavage sites are not used at the same frequencies. The cleavage site located 22 bases downstream of the PAS represents 78% of the *DUX4-FL1* isoforms but only 41% of *DUX4-FL2* isoforms thus showing the interplay between mRNA cleavage site and splicing (Fig. 1A-B). In order to investigate the therapeutic potential of AONs targeting 3' key elements of *DUX4* mRNA, we designed AONs covering either the PAS (PMO-PAS), the cleavage sites and the polyA (PMO-CS1 to 3) or the U/GU-rich (PMO-DSE) sequence (Fig. 1C). Briefly, PMOs were designed to (i) contain little or no self-complementarity (ii) form no more than 16 contiguous intrastrand hydrogen bonds (iii) contain no more than 9 total guanines (>36% G) or more than 3 contiguous guanines to ensure good water solubility, and (iv) where possible to target more than one of the 3' key elements with one PMO. For these reasons, the cleavage site PMOs contains either a single mismatch to target (PMO-CS2 and PMO-CS3) or do not target contiguous bases (PMO-CS1). These PMOs were of varying lengths (25mers to 30mers) (Table 1).

PMOs induce a down expression of *DUX4* mRNA

The efficacy of each PMO was evaluated in a dose dependent manner after transfection into differentiated immortalized FSHD clones. Total RNAs were extracted from myotubes and RT-PCR allowing the detection of either *DUX4-all* (Fig. 2A), or *DUX4-FL1* and -*FL2* (Fig. 2B) was performed. No modification of *DUX4-all* mRNA was observed with PMO-control compared to unlipofected cells thus showing that introduction of PMO-control does not modify *DUX4* expression. With PMO-CS1, –CS2 and -DSE, 27% +/- 5, 25% +/- 17and 36% +/- 10 reduction of *DUX4-all* mRNA was observed respectively at the highest PMO

concentration used compared with PMO-control (Fig. 2A). The highest efficacies were obtained with the PMO-PAS and –CS3 for which a dose-dependent reduction of *DUX4-all* levels was observed with 40% +/- 6 and 52% +/- 7 inhibition at 50nM respectively (Fig. 2A). These two antisense oligonucleotides were investigated further to ascertain if both *DUX4* isoforms were identically targeted by them. A decreased expression of both isoforms was observed at 50nM when primers allowing the detection of both *DUX4-FL1* and *FL-2* (DUX4-3'UTR oligonucleotides) were used (Fig. 2B).

PMO-CS3 induces a redirection of cleavage region

Because 22 to 54% of human mRNA have more than one poly(A) sites (4, 5), and because redirections of the poly(A) signal have been described in the presence of antisense oligonucleotides targeting the poly(A) of other mRNAs (44, 45), *in silico* analyses were performed which revealed the presence of putative alternative poly(A) signal downstream of exon 3 (Fig. 3A). A redirection of the poly(A) and/or cleavage sites was thus investigated in the presence of the different PMOs at the highest concentration by 3'RACE nested PCR using forward primers located in exon 3. A switch in cleavage site or poly(A) usage was not observed with any of the PMOs except PMO-CS3 (Fig. 3B). The sequence of this supplemental band revealed that the cleavage site of the residual *DUX4* mRNA in the presence of PMO-CS3 was ~40 nt upstream of the canonical cleavage site (Fig. 3C), thus suggesting that an alternative poly(A) signal was used to generate this new cleavage site. However, i*n silico* analysis of the genomic region upstream of this alternative cleavage site (up to *DUX4* exon2) did not reveal the presence of any of the 13 PAS previously described (4). This new cleavage site is used in approximatively 20% of the residual *DUX4* mRNAs.

PMO-PAS and –CS3 induce a knockdown in expression of genes downstream of DUX4 in FSHD cells

Because DUX4 protein is very hard to detect, expression levels of DUX4 biomarkers were investigated. Indeed, DUX4 being a transcription factor, the expression levels of several genes downstream of DUX4 have been described to be modulated after DUX4 expression among them *TRIM43*, *MBD3L2* and *ZSCAN4* (21, 27, 46). the expression of these three genes was determined by RT-qPCR in the presence of the PMOs in a dose dependent manner. No significant modulation of their expressions was observed in the presence of PMO-control compared to unlipofected condition. PMO-CS1, -CS2 and –DSE moderately modulate expression of genes downstream of DUX4 at the lowest concentrations used but a down expression of *TRIM43* is observed at the highest concentration. The best modulation of the genes downstream of DUX4 was observed in the presence of PMO-PAS and –CS3 in a dose dependent manner (Fig. 4).

Since we have previously published that DUX4 is able to spread from one FSHD nucleus to neighboring nuclei thus inducing an aberrant activation of genes downstream of DUX4 in many nuclei (23), one possible explanation for the lower expression of *TRIM43*, *MBD3L2* and *ZSCAN4* observed in the presence of the PMO-PAS and –CS3 could have been an inhibition of myotube formation mediated by the PMOs. PMO-transfected cells were immunostained with the MF20 antibody recognizing all the myosin heavy chains (Fig. 5A) and fusion indexes were calculated by counting the number of nuclei in MF20-positive myotubes containing 3 or more nuclei as the percentage of total number of nuclei (Fig. 5B). No statistically significant differences were observed with PMO treatment thus showing that the downregulation of the genes downstream of DUX4 in the presence of the PMOs was not due to myotube formation impairment but rather to lowered DUX4 expression.

No significant off-targets are predicted

The potential off-target effects were also evaluated, PMOs targeting the *DUX4* transcript were submitted to short-input-sequence BLAST searches against coding and non-coding human genome nucleotide collection databases (nr/nr and nr/nt: see Table 3). According to BLAST a very strong match is considered to have E-value of <1e-04, whereas a poor match has E-value >1e-03. For each PMO, the two BLAST returns showing highest alignment scores (lowest E-values) were selected for further analysis. With the exception of PMO-CS1 which contains specifically selected deletions, all designed PMOs returned a very strong match to the desired *DUX4* transcript (E-value ≤ 2e-05), whereas all of the off-target gene candidates show high E-values >0.5. Predicted off-target sequence matches that showed homology on their negative or forward strand, corresponding to RNA transcript, were selected for calculation of total free energy of binding using the RNAup Server (Table 3; Supplementary figure S1). The only potential off-target interactions on the RNA transcript (ie negative strand) was GYS2 for PMO-PAS and PTPRT for PMO-CS1, but overall free energies of binding were low (-16.62 and -6.60 respectively), and with major mismatches (8/21 and 12/29, respectively). These data suggest a low probability of interference of any of the designed PMOs targeting *DUX4* with off target RNAs.

DISCUSSION

Several strategies using antisense oligonucleotides have been described during the last decade. Upon binding, AOs can alter the original function of the targeted mRNA through an array of different mechanisms. In the literature, AOs have been described to (i) prevent 5'cap formation, (ii) bind the pre-mRNA to modulate splicing by masking the splicing sequences to force exon inclusion or exclusion, (iii) induce mRNA degradation after the recognition of the duplex AO-mRNA (depending on the chemical modification used), (iv) inhibit ribosome

access to the mRNA leading to the suppression of protein translation, (v) modulate polyadenylation selection in transcripts with more than one poly(A) in their 3'UTR (for review see (39)). However, to our knowledge, the possibility to target the 3'UTR key elements of the mammalian pre-mRNA to inhibit the polyadenylation in genetic diseases has not been studied.

As previously described, defects in mRNA 3' end formation can result in disruption of gene expression processes in a number of ways, including: transcription termination; transport of the mRNA from the nucleus to the cytoplasm; stability of the mRNA; translation efficiency and the inhibition of polyadenylation, which in turn might lead to gene silencing (for review see (47)). In this study we investigate the possibility of interference in the 3'end mRNA processing as a therapeutic approach in the FSHD model. Since FSHD is a gain of function disease, characterized by the aberrant over-expression of the *DUX4* gene, the therapeutic strategies should therefore be based on gene silencing rather than gene rescue. Here we show that targeting the 3' end elements involved in mRNA processing is an effective way to decrease *DUX4* expression and prevent aberrant expression of genes downstream of DUX4.

Among the 5 AONs tested, only 2 of them lead to a significant decrease of *DUX4* mRNA levels under the conditions evaluated. PMOs length could play an important role in their efficacies, since PMO-CS3 is the only 30-mer used in this study and is the antisens oligonucleotide showing the best efficiency. The number of mismatches could also play a role affecting their relative activity when compared to a completely homologous sequence of equal length. Secondary structures may also have affected effectiveness of the PMOs and secondary structures of exon 3 of *DUX4* or the AON were analyzed *in silico* using thermodynamic methods. Indeed, the probability of interaction between the AON and the targeted mRNA can be impacted by the presence of closed or opened conformations at the site of hybridization (47). When calculating the minimum free energy of a folded mRNA molecule using mfold

(http://mfold.rna.albany.edu/?q=mfold/RNA-Folding-Form2.3) (48, 49), the exon 3 of *DUX4* was predicted to form highly stable secondary structure with free energies of – 56.3 kcal/mol (Fig. 6). The resulting outputs show that *DUX4* poly(A) is located within the region of an open confirmation, whereas the cleavage site and the DSE lay within a closed region. The PAS thus appears more accessible than the DSE and this could explain the low efficacy of the PMO-DSE which totally overlap a closed region.

Different mechanisms may be involved in the down-regulation of the targeted mRNA in the presence of the PMOs. The first one is that the duplex formation of the PMO with the mRNA 3'UTR could prevent poly(A) tail elongation. The second one could be the removal of the entire tail mediated by a deadenylase-dependent cutting of the poly(A) tail as previously described in zebrafish (50), thus affecting mRNA stability. Another possibility is that spatial rearrangements of the 3'UTR in the presence of the PMO could have modulated the nonsense mediated decay (NMD) pathway (51). In one hand, it was previously shown that NMD is an endogenous suppressor of *DUX4* mRNA that contributes to the low expression of *DUX4* in FSHD cells (30). But in the other hand, DUX4 expression was also described to inhibit NMD by decreasing UPF1 levels (30). The PMO-*DUX4* duplex formation, causing a destabilization of *DUX4* mRNA by at least one of the mechanisms described earlier, could have thus increased NMD activity, enhancing *DUX4* repression.

Recent discoveries have revealed that many human genes use more than one poly(A) and cleavage sites, indicating that alternative polyadenylation (APA) is a widespread phenomenon. The use of APA has been described to play important roles in several human diseases such as (i) in Oculopharyngeal muscular dystrophy (OPMD), in which mutations in PABPN1 result in a global enhancement of usage of proximal cleavage sites, leading to an unbalanced formation of alternative mRNA 3'ends and to a modification of gene expression through aberrant microRNA regulation (52); (ii) in β–thalassemia, in which a loss-of-function

of globin 3' end processing linked to an alteration of the poly(A) site is one of the causes of this disease, resulting in the generation of an unstable transcript that is ~900 nt longer (for reviews see (1, 7)); (iii) a single nucleotide polymorphism in the U/GU rich region downstream of an alternative poly(A) signal in the Fibrinogen gamma haplotype 2 (FGG-H2) gene has been shown to affect the usage of this poly(A) and has been associated with increased risk of deep-venous thrombosis (53). Considering that the use of antisens oligonucleotides targeting the poly(A) site can lead to the use of APA and cleavage site (44, 45), one important point raised in our experiments was to determine if such a redirection was observed in the presence of the PMOs. Although in the presence of PMO-CS3 the cleavage site was detected to be redirected by ~40 nt upstream of its normal position, it was still considerably distal to any of the previously described alternative poly(A) signals (4). Interestingly, this finding does not fit with the current consensus describing that there are 4 general classes of APA, including: tandem 3'UTR APA; alternative terminal exon APA; intronic APA; and internal exon APA (1). This could be explained by the steric congestion at the PAS and cleavage site provided by the PMO-CS3 and the cellular proteins involved in the polyadenylation process, respectively. The cleavage factors would be then forced to cleave the pre-mRNA upstream of the poly(A) signal, resulting in a new cleavage site but still utilizing the original poly(A) site. Importantly, in the 14 sequences analyzes, the same cleavage region was observed, strongly suggesting a specificity to the target sequence. Alternatively, a novel APA was used that has not been previously described (4).

A redirection of the cleavage site associated to the alternative poly(A) site located in exon 7 of *DUX4* was not observed either. It was shown that chromosomes 4 and 10 produce *DUX4* mRNA in human testes (18). These transcripts can use alternative 3' exons with a poly(A) signal in exon 7, leading to a *DUX4* mRNA carrying exons 1-2-6-7 or exons 1-2-4-5-6-7.

Exons 3 and 7 thus seem to be mutually exclusive. It is therefore not surprising to not observe a redirection of the cleavage site to exon 7 when exon 3 is targeted.

Targeting the 3'end elements of mRNA could thus represent an alternative approach for gene silencing compared to classic antisense oligonucleotide approaches leading to exon skipping, translation inhibition, or mRNA destruction into the cytoplasm. The strategy to interfere with the mRNA 3' end processing provides a number of advantages. First, polyadenylation is a crucial step required for the maturation of almost all eukaryotic mRNAs (except for histones), meaning that virtually any mRNA can be subjected to this strategy. Second, genes with only 1 exon can be targeted using AON hybridizing the 3'end key elements. Third, AON targeting the poly(A) signals may be investigated in a therapeutic context for some disease caused by utilization of inadequate APAs. For example, some mantle cell lymphoma patients express isoforms of *cyclinD1* mRNA with short 3'UTR compared to healthy individuals. Shortening of the 3'UTR is caused by the mutations in the *CCND1* gene leading to the creation of a premature poly(A) signal. This mutated mRNA lacks most of the 3'UTR region that contains mRNA destabilizing elements, making the *CCDN1* mRNA abnormally stable (54). Therefore targeting a premature poly(A) with AON to promote the use of the distal poly(A) may also serve as an promising approach to treat disease.

MATERIAL AND METHODS

PMO were manufactured and supplied by Gene Tools (LLC, Philomath, USA). The DNA leashes for PMO transfection were synthesized by Eurogentec and their sequences are indicated in table 1. Before transfection, the PMOs (2.5 µl at 1 mM) were annealed with the leash (25 µl at100 µM) in final volume of 50µL (12.5µL of PBS10X and 10µL of RNAse-free water) (final concentration of leashed PMO 50 µM) using the following protocol: 95ºC for

5min, 85ºC for 1min, 75ºC for 1min, 65ºC for 5min, 55ºC for 1min, 45ºC for 1min, 35ºC for 5min, 25ºC for 1min and then held at 15ºC. Efficient annealing was verified using gel electrophoresis band shift as previously described (55). Leashed PMOs were stored at 4ºC.

Immortalized FSHD clones have been characterized previously (56). Cells were cultivated in proliferation medium [4 vols of DMEM (Dulbecco's modified Eagle medium), 1 vol of 199 medium, FBS (Fetal Bovine Serum) 20%, gentamycin 50µg/mL (Life Technologies, Saint Aubin, France)] supplemented with insulin 5µg/mL, dexamethasone 0.2µg/mL, β-FGF 0.5ng/mL, hEGF 5ng/ml and fetuine 25µg/mL. The differentiation was induced by replacing the proliferation medium by DMEM supplemented with insulin (10µg/mL). Two days after the induction of differentiation, the transfections were realized using Lipofectamine® RNAiMax Reagent (Life Technologies) according to the manufacturer's instructions. Cells were harvested at day 4 of differentiation.

RNA extraction from cultured cells was performed using Trizol according the manufacturer's protocol (Life Technologies, Saint Aubin, France). RNA concentration was determined using a nanodrop ND-1000 spectrophotometer (Thermo Scientific, Wilmington, USA). Reverse transcription was performed on 1µg of total RNA in 10µl final volume (Roche Transcriptor First Strand cDNA Synthesis Kit, Roche, Meylan, France) with a NVT primer (GCGAGCTCCGCGGCCGCGTTTTTTTTTTVN) (10µM) according to the manufacturer instructions. The PCR for *DUX4-all* was performed on 1µL of cDNA using 2X Reddy Mix PCR Master Mix (Thermo Scientific) according the manufacturer's instructions. The PCR program was the following: 94ºC for 5min, followed by 35 cycles at 94ºC for 20 s and 60ºC for 20 s and 72ºC for 20s, finished with 72ºC for 7min. Quantitative PCR (qPCR) was designed according to the MIQE standards (57). The primers used for both PCR and qPCR are indicated in table 2. Quantitative PCRs were performed in a final volume of 9µL with 4µL of RT product, 0.18µL of each forward and reverse primers at 20µM, and 4.5µL of SYBR®

Green mastermix 2X (Roche, Meylan, France) in a lightcycler LC480 (Roche). The qPCR cycling conditions were 94ºC for 5min, followed by 50 cycles at 94ºC for 10s and 60ºC for 5s and 72ºC for 5s. All the amplicons were validated using sequencing. *B2M* was the most appropriate gene for normalization: a multiparametric analysis of variance (MANOVA) and a Newman-Keuls post-hoc test did not reveal any correlation between *B2M* expression and PMO addition (at different concentrations).

For the 3'RACE, the RT was realized with an oligo dT adapter primer: (GCTGTCAACGATACGCTACGTAACGGCATGACAGTGTTTTTTTTTTTTTTTTTT TTTT) as described in table 2. The primary PCRs were performed in a final volume of 15µL with 1uL of RT product, 3µL of reverse primer at 20µM (Table 2) and 1µL of primer at 20µM, 7.5µL 2X ReddyMix PCR Master Mix (Thermo Scientific). The PCR cycling conditions were 94ºC for 5min, followed by 5 cycles at 94ºC for 20 s and 72ºC for 50 s, then 5 cycles at 94ºC for 20s and 70ºC for 30s and 72ºC for 20s, and 25 cycles at 94ºC for 20s and 68ºC for 20s and 72ºC for 30s, finished with 72ºC for 7min. The nested PCRs were realized in a final volume of 15µL with 1µL of primary PCR product, 1µL of reverse and/or forward primers 20µM, 7.5µL 2X ReddyMix PCR Master Mix (Thermo Scientific). The PCR cycling conditions were 94ºC for 5min, followed by 35 cycles at 94ºC for 20s and 60ºC for 20s and 72ºC for 30s, finished with 72ºC for 7min. Nested PCR products were purified according Nucleospin Gel and PCR Clean Up manufacturer instructions (Macherey-Nagel). Fragments were cloned into TOPO TA vector with TOPO TA Cloning kit (Lifetechnologies). Cleavage sites were determined by sequencing at least 10 colony-forming units.

ACKNOWLEDGEMENTS

This study was financially supported by the French Association against Myopathies (AFM-Téléthon, France) and the National Research Agency (FSHDecipher, ANR-13-BSV1-0004) and The Rosetrees Trust, UK.

CONFLICT OF INTEREST STATEMENT: none declared

REFERENCES

1. Elkon, R., Ugalde, A.P. and Agami, R. (2013) Alternative cleavage and polyadenylation: extent, regulation and function. *Nature reviews,* **14,** 496-506.

2. Nunes, N.M., Li, W., Tian, B. and Furger, A. (2010) A functional human Poly(A) site requires only a potent DSE and an A-rich upstream sequence. *The EMBO journal,* **29,** 1523-1536.

3. Proudfoot, N.J. (2011) Ending the message: poly(A) signals then and now. *Genes & development,* **25,** 1770-1782.

4. Tian, B., Hu, J., Zhang, H. and Lutz, C.S. (2005) A large-scale analysis of mRNA polyadenylation of human and mouse genes. *Nucleic acids research,* **33,** 201-212.

5. Beaudoing, E., Freier, S., Wyatt, J.R., Claverie, J.M. and Gautheret, D. (2000) Patterns of variant polyadenylation signal usage in human genes. *Genome research,* **10,** 1001-1010.

6. Gruber, A.R., Martin, G., Keller, W. and Zavolan, M. (2014) Means to an end: mechanisms of alternative polyadenylation of messenger RNA precursors. *Wiley interdisciplinary reviews,* **5,** 183-196.

7. Danckwardt, S., Hentze, M.W. and Kulozik, A.E. (2008) 3' end mRNA processing: molecular mechanisms and implications for health and disease. *The EMBO journal,* **27,** 482-498.

8. Sachs, A. (1990) The role of poly(A) in the translation and stability of mRNA. *Current opinion in cell biology,* **2,** 1092-1098.

9. Hollerer, I., Grund, K., Hentze, M.W. and Kulozik, A.E. (2014) mRNA 3'end processing: A tale of the tail reaches the clinic. *EMBO molecular medicine,* **6,** 16-26.

10. Tawil, R., van der Maarel, S.M. and Tapscott, S.J. (2014) Facioscapulohumeral dystrophy: the path to consensus on pathophysiology. *Skeletal muscle,* **4,** 12.

11. van der Maarel, S.M., Miller, D.G., Tawil, R., Filippova, G.N. and Tapscott, S.J. (2012) Facioscapulohumeral muscular dystrophy: consequences of chromatin relaxation. *Current opinion in neurology,* **25,** 614-620.

12. van Deutekom, J.C., Wijmenga, C., van Tienhoven, E.A., Gruter, A.M., Hewitt, J.E., Padberg, G.W., van Ommen, G.J., Hofker, M.H. and Frants, R.R. (1993) FSHD associated DNA rearrangements are due to deletions of integral copies of a 3.2 kb tandemly repeated unit. *Human molecular genetics,* **2,** 2037-2042.

13. Wijmenga, C., Hewitt, J.E., Sandkuijl, L.A., Clark, L.N., Wright, T.J., Dauwerse, H.G., Gruter, A.M., Hofker, M.H., Moerer, P., Williamson, R. *et al.* (1992) Chromosome 4q DNA rearrangements associated with facioscapulohumeral muscular dystrophy. *Nature genetics,* **2,** 26-30.

14. Lemmers, R.J., Tawil, R., Petek, L.M., Balog, J., Block, G.J., Santen, G.W., Amell, A.M., van der Vliet, P.J., Almomani, R., Straasheijm, K.R. *et al.* (2012) Digenic inheritance of an SMCHD1 mutation and an FSHD-permissive D4Z4 allele causes facioscapulohumeral muscular dystrophy type 2. *Nature genetics,* **44,** 1370-1374.

15. Lemmers, R.J., van den Boogaard, M.L., van der Vliet, P.J., Donlin-Smith, C.M., Nations, S.P., Ruivenkamp, C.A., Heard, P., Bakker, B., Tapscott, S., Cody, J.D. *et al.* (2015) Hemizygosity for SMCHD1 in Facioscapulohumeral Muscular Dystrophy Type 2: Consequences for 18p Deletion Syndrome. *Human mutation,* **36,** 679-683.

16. Lemmers, R.J., van der Vliet, P.J., Klooster, R., Sacconi, S., Camano, P., Dauwerse, J.G., Snider, L., Straasheijm, K.R., van Ommen, G.J., Padberg, G.W. *et al.* (2010) A unifying genetic model for facioscapulohumeral muscular dystrophy. *Science* **329,** 1650-1653.

17. Snider, L., Asawachaicharn, A., Tyler, A.E., Geng, L.N., Petek, L.M., Maves, L., Miller, D.G., Lemmers, R.J., Winokur, S.T., Tawil, R. *et al.* (2009) RNA transcripts, miRNA-sized fragments and proteins produced from D4Z4 units: new candidates for the pathophysiology of facioscapulohumeral dystrophy. *Human molecular genetics,* **18,** 2414-2430.

18. Snider, L., Geng, L.N., Lemmers, R.J., Kyba, M., Ware, C.B., Nelson, A.M., Tawil, R., Filippova, G.N., van der Maarel, S.M., Tapscott, S.J. *et al.* (2010) Facioscapulohumeral dystrophy: incomplete suppression of a retrotransposed gene. *PLoS genetics,* **6,** e1001181.

19. Jones, T.I., Chen, J.C., Rahimov, F., Homma, S., Arashiro, P., Beermann, M.L., King, O.D., Miller, J.B., Kunkel, L.M., Emerson, C.P., Jr. *et al.* (2012) Facioscapulohumeral muscular dystrophy family studies of DUX4 expression: evidence for disease modifiers and a quantitative model of pathogenesis. *Human molecular genetics,* **21,** 4419-4430.

20. Broucqsault, N., Morere, J., Gaillard, M.C., Dumonceaux, J., Torrents, J., Salort-Campana, E., Maues de Paula, A., Bartoli, M., Fernandez, C., Chesnais, A.L. *et al.* (2013) Dysregulation of 4q35- and muscle-specific genes in fetuses with a short D4Z4 array linked to Facio-Scapulo-Humeral Dystrophy. *Human molecular genetics,* **22,** 4206-4214.

21. Ferreboeuf, M., Mariot, V., Bessieres, B., Vasiljevic, A., Attie-Bitach, T., Collardeau, S., Morere, J., Roche, S., Magdinier, F., Robin-Ducellier, J. *et al.* (2014) DUX4 and DUX4 downstream target genes are expressed in fetal FSHD muscles. *Human molecular genetics,* **23,** 171-181.

22. Block, G.J., Narayanan, D., Amell, A.M., Petek, L.M., Davidson, K.C., Bird, T.D., Tawil, R., Moon, R.T. and Miller, D.G. (2013) Wnt/beta-catenin signaling suppresses DUX4

expression and prevents apoptosis of FSHD muscle cells. *Human molecular genetics,* **22,** 390-396.

23. Ferreboeuf, M., Mariot, V., Furling, D., Butler-Browne, G., Mouly, V. and Dumonceaux, J. (2014) Nuclear protein spreading: implication for pathophysiology of neuromuscular diseases. *Human molecular genetics,* **23,** 4125-4133.

24. Kowaljow, V., Marcowycz, A., Ansseau, E., Conde, C.B., Sauvage, S., Matteotti, C., Arias, C., Corona, E.D., Nunez, N.G., Leo, O. *et al.* (2007) The DUX4 gene at the FSHD1A locus encodes a pro-apoptotic protein. *Neuromuslar Disorders,* **17,** 611-623.

25. Dixit, M., Ansseau, E., Tassin, A., Winokur, S., Shi, R., Qian, H., Sauvage, S., Matteotti, C., van Acker, A.M., Leo, O. *et al.* (2007) DUX4, a candidate gene of facioscapulohumeral muscular dystrophy, encodes a transcriptional activator of PITX1. *Proceedings of the National Academy of Sciences of the United States of America,* **104,** 18157-18162.

26. Wallace, L.M., Garwick, S.E., Mei, W., Belayew, A., Coppee, F., Ladner, K.J., Guttridge, D., Yang, J. and Harper, S.Q. (2011) DUX4, a candidate gene for facioscapulohumeral muscular dystrophy, causes p53-dependent myopathy in vivo. *Annals of neurology,* **69,** 540-552.

27. Geng, L.N., Yao, Z., Snider, L., Fong, A.P., Cech, J.N., Young, J.M., van der Maarel, S.M., Ruzzo, W.L., Gentleman, R.C., Tawil, R. *et al.* (2012) DUX4 Activates Germline Genes, Retroelements, and Immune Mediators: Implications for Facioscapulohumeral Dystrophy. *Dev Cell,* **22,** 38-51.

28. Xu, H., Wang, Z., Jin, S., Hao, H., Zheng, L., Zhou, B., Zhang, W., Lv, H. and Yuan, Y. (2014) Dux4 induces cell cycle arrest at G1 phase through upregulation of p21 expression. *Biochemical and biophysical research communications,* **446,** 235-240.

29. Rickard, A.M., Petek, L.M. and Miller, D.G. (2015) Endogenous DUX4 expression in FSHD myotubes is sufficient to cause cell death and disrupts RNA splicing and cell migration pathways. *Human molecular genetics,* **24,** 5901-5914.

30. Feng, Q., Snider, L., Jagannathan, S., Tawil, R., van der Maarel, S.M., Tapscott, S.J. and Bradley, R.K. (2015) A feedback loop between nonsense-mediated decay and the retrogene DUX4 in facioscapulohumeral muscular dystrophy. *eLife,* **4**.

31. Tupler, R., Berardinelli, A., Barbierato, L., Frants, R., Hewitt, J.E., Lanzi, G., Maraschio, P. and Tiepolo, L. (1996) Monosomy of distal 4q does not cause facioscapulohumeral muscular dystrophy. *Journal of Medical Genetics,* **33,** 366-370.

32. Lemmers, R.J., de Kievit, P., Sandkuijl, L., Padberg, G.W., van Ommen, G.J., Frants, R.R. and van der Maarel, S.M. (2002) Facioscapulohumeral muscular dystrophy is uniquely associated with one of the two variants of the 4q subtelomere. *Nature genetics,* **32,** 235-236.

33. Thomas, N.S., Wiseman, K., Spurlock, G., MacDonald, M., Ustek, D. and Upadhyaya, M. (2007) A large patient study confirming that facioscapulohumeral muscular dystrophy (FSHD) disease expression is almost exclusively associated with an FSHD locus located on a 4qA-defined 4qter subtelomere. *Journal of Medical Genetics,* **44,** 215-218.

34. Yao, Z., Snider, L., Balog, J., Lemmers, R.J., Van Der Maarel, S.M., Tawil, R. and Tapscott, S.J. (2014) DUX4-induced gene expression is the major molecular signature in FSHD skeletal muscle. *Human molecular genetics,* **23,** 5342-5352.

35. Wallace, L.M., Liu, J., Domire, J.S., Garwick-Coppens, S.E., Guckes, S.M., Mendell, J.R., Flanigan, K.M. and Harper, S.Q. (2012) RNA Interference Inhibits DUX4-induced Muscle Toxicity In Vivo: Implications for a Targeted FSHD Therapy. *Molecular Therapy,* **20,** 1417-1423.

36. Mitsuhashi, H., Mitsuhashi, S., Lynn-Jones, T., Kawahara, G. and Kunkel, L.M. (2013) Expression of DUX4 in zebrafish development recapitulates facioscapulohumeral muscular dystrophy. *Human molecular genetics,* **22,** 568-577.

37. Vanderplanck, C., Ansseau, E., Charron, S., Stricwant, N., Tassin, A., Laoudj-Chenivesse, D., Wilton, S.D., Coppee, F. and Belayew, A. (2011) The FSHD Atrophic Myotube Phenotype Is Caused by DUX4 Expression. *PloS one,* **6,** e26820.

38. Kole, R., Krainer, A.R. and Altman, S. (2012) RNA therapeutics: beyond RNA interference and antisense oligonucleotides. *Nature Reviews Drug Discovery,* **11,** 125-140.

39. DeVos, S.L. and Miller, T.M. (2013) Antisense oligonucleotides: treating neurodegeneration at the level of RNA. *Neurotherapeutics,* **10,** 486-497.

40. Cirak, S., Arechavala-Gomeza, V., Guglieri, M., Feng, L., Torelli, S., Anthony, K., Abbs, S., Garralda, M.E., Bourke, J., Wells, D.J. *et al.* (2011) Exon skipping and dystrophin restoration in patients with Duchenne muscular dystrophy after systemic phosphorodiamidate morpholino oligomer treatment: an open-label, phase 2, dose-escalation study. *The Lancet,* **378,** 595-605.

41. Mendell, J.R., Rodino-Klapac, L.R., Sahenk, Z., Roush, K., Bird, L., Lowes, L.P., Alfano, L., Gomez, A.M., Lewis, S., Kota, J. *et al.* (2013) Eteplirsen for the treatment of Duchenne muscular dystrophy. *Annals of neurology,* **74,** 637-647.

42. Jarmin, S., Kymalainen, H., Popplewell, L. and Dickson, G. (2013) New developments in the use of gene therapy to treat Duchenne muscular dystrophy. *Expert opinion on biological therapy,* **14,** 209-230.

43. Voit, T., Topaloglu, H., Straub, V., Muntoni, F., Deconinck, N., Campion, G., De Kimpe, S.J., Eagle, M., Guglieri, M., Hood, S. *et al.* (2014) Safety and efficacy of drisapersen for the treatment of Duchenne muscular dystrophy (DEMAND II): an exploratory, randomised, placebo-controlled phase 2 study. *The Lancet,* **13,** 987-996.

44. Raz, V., Buijze, H., Raz, Y., Verwey, N., Anvar, S.Y., Aartsma-Rus, A. and van der Maarel, S.M. (2014) A novel feed-forward loop between ARIH2 E3-ligase and PABPN1 regulates aging-associated muscle degeneration. *The American journal of pathology,* **184,** 1119-1131.

45. Vickers, T.A., Wyatt, J.R., Burckin, T., Bennett, C.F. and Freier, S.M. (2001) Fully modified 2' MOE oligonucleotides redirect polyadenylation. *Nucleic acids research,* **29,** 1293-1299.

46. Mariot, V., Roche, S., Hourde, C., Portilho, D., Sacconi, S., Puppo, F., Duguez, S., Rameau, P., Caruso, N., Delezoide, A.L. *et al.* (2015) Correlation between low FAT1 expression and early affected muscle in facioscapulohumeral muscular dystrophy. *Annals of neurology,* **78,** 387-400.

47. Millevoi, S. and Vagner, S. (2010) Molecular mechanisms of eukaryotic pre-mRNA 3' end processing regulation. *Nucleic acids research,* **38,** 2757-2774.

48. Zuker, M. (2003) Mfold web server for nucleic acid folding and hybridization prediction. *Nucleic acids research,* **31,** 3406-3415.

49. Wu, J.C., Gardner, D.P., Ozer, S., Gutell, R.R. and Ren, P. (2009) Correlation of RNA secondary structure statistics with thermodynamic stability and applications to folding. *Journal of molecular biology,* **391,** 769-783.

50. Wada, T., Hara, M., Taneda, T., Qingfu, C., Takata, R., Moro, K., Takeda, K., Kishimoto, T. and Handa, H. (2012) Antisense morpholino targeting just upstream from a poly(A) tail junction of maternal mRNA removes the tail and inhibits translation. *Nucleic acids research,* **40,** e173.

51. Eberle, A.B., Stalder, L., Mathys, H., Orozco, R.Z. and Muhlemann, O. (2008) Posttranscriptional gene regulation by spatial rearrangement of the 3' untranslated region. *PLoS Biol,* **6,** e92.

52. Jenal, M., Elkon, R., Loayza-Puch, F., van Haaften, G., Kuhn, U., Menzies, F.M., Oude Vrielink, J.A., Bos, A.J., Drost, J., Rooijers, K. *et al.* (2012) The poly(A)-binding protein nuclear 1 suppresses alternative cleavage and polyadenylation sites. *Cell,* **149,** 538-553.

53. Uitte de Willige, S., Rietveld, I.M., De Visser, M.C., Vos, H.L. and Bertina, R.M. (2007) Polymorphism 10034C>T is located in a region regulating polyadenylation of FGG transcripts and influences the fibrinogen gamma'/gammaA mRNA ratio. *Journal of Thrombosis and Haemostasis,* **5,** 1243-1249.

54. Wiestner, A., Tehrani, M., Chiorazzi, M., Wright, G., Gibellini, F., Nakayama, K., Liu, H., Rosenwald, A., Muller-Hermelink, H.K., Ott, G. *et al.* (2007) Point mutations and genomic deletions in CCND1 create stable truncated cyclin D1 mRNAs that are associated with increased proliferation rate and shorter survival. *Blood,* **109,** 4599-4606.

55. Popplewell, L.J., Graham, I.R., Malerba, A. and Dickson, G. (2011) Bioinformatic and functional optimization of antisense phosphorodiamidate morpholino oligomers (PMOs) for therapeutic modulation of RNA splicing in muscle. *Methods in Molecular Biology,* **709,** 153-178.

56. Krom, Y.D., Dumonceaux, J., Mamchaoui, K., den Hamer, B., Mariot, V., Negroni, E., Geng, L.N., Martin, N., Tawil, R., Tapscott, S.J. *et al.* (2012) Generation of isogenic D4Z4 contracted and noncontracted immortal muscle cell clones from a mosaic patient: a cellular model for FSHD. *The American journal of pathology,* **181,** 1387-1401.

57. Bustin, S.A., Benes, V., Garson, J.A., Hellemans, J., Huggett, J., Kubista, M., Mueller, R., Nolan, T., Pfaffl, M.W., Shipley, G.L. *et al.* (2009) The MIQE guidelines: minimum information for publication of quantitative real-time PCR experiments. *Clinical chemistry,* **55,** 611-622.

FIGURES LEGENDS

Figure 1: 3'end key elements of *DUX4* mRNA and PMO design.

A and B: To determine the cleavage sites of *DUX4* mRNA, a RT using an oligo dT adapter primer was realized on total mRNAs isolated from FSHD myotubes at day 4 of differentiation. The 3'RACE-PCR was performed using forward primer matching exon 1 and reverse primer recognizing the adapter. The PCR products were cloned into a TOPO-TA plasmid and 27 and 17 clones were sequenced for *DUX4-FL1* (A) and *–FL2* (B) respectively. The frequencies of the cleavage site usages are indicated. Arrows indicate the location of the primers used. The poly(A) site is bolded and underlined and the poly(A) tail is in bold.

C: Sequences recognized by the different PMOs targeting *DUX4*. The position +1 is defined as the first base of the poly(A) site. The sequences recognized by the PMOs are indicated as well as their position on the mRNA. Deletions are represented by hyphen (-). Nucleotidic substitutions are indicated.

Figure 2: *DUX4* expression in the presence of the PMOs

Immortalized FSHD myotubes were transfected with PMOs in a dose dependent manner. (A) The percentage of residual *DUX4-all* mRNA was measured by semi quantitative PCR using ImageJ software on gel scans. Independent transfections for PMO-control, -PAS, -CS1, -CS2, CS3, and -DSE ($n \geq 6$) were performed. Values are compared to unlipofected conditions. All data represent mean +/- Standard Error of Mean (SEM). A multiparametric analysis of variance and a Newman–Keuls post hoc test were performed (*$p<0.05$; **$p<0.01$; ***$p<0.001$). (B): Representative RT-PCR analysis using *DUX4-3'UTR* primers in the presence of PMO-control, PAS, and -CS3 at 50 nM. As a negative control, a PMO targeting a human β-globin mutation that causes β-thalassemia was be used. *B2M* was used as the reference (housekeeping) gene.

Figure 3: PMO-CS3 induces a switch in cleavage site usage.

A redirection of poly(A) usage was investigated in the presence of the different PMOs. (A) *In silico* analyses and literature (18) reveal the presence of alternative polyadenylation site in the subtelomeric region of chromosome 4. (B) 3'RACE nested PCR using forward primers located in exon 3 shows a switch in cleavage site only in the presence of PMO-CS3. The bands with (**) or without (*) a redirection of the cleavage site are indicated. (C) Sequence of the most abundant mRNA carrying the redirected cleavage site (*DUX4* pre-mRNA). The sequence of poly(A) site is underlined and bolded. The poly(A) tail is in bold. The frequencies of each variant showing alternative cleavage site usage are indicated (14 analyzed sequences).

Figure 4: Expression of the genes downstream of DUX4 in presence of the PMOs

Expression levels of *TRIM43* (A), *ZSCAN4* (B) and *MBD3L2* (C) were measured by RT-qPCR in FSHD myotubes (4 days of differentiation) in the presence of the PMOs at different concentrations and compared to the PMO control at the same concentration. Values are compared to unlipofected conditions. *B2M* was used as a normalizer. Data represent mean +/- standard error of mean from independent transfections for PMO-control, -PAS, -CS1, -CS2, CS3, and -DSE ($n \geq 6$). A multiparametric analysis of variance and a Newman–Keuls post hoc test were performed (*$p<0.05$; **$p<0.01$; ***$p<0.001$).

Figure 5: Fusion index of immortalized FSHD myotubes in the presence of the PMOs

Immortalized FSHD myotubes were transfected at day 2 of differentiation with the different PMOs at 50 nM. At day 4 of differentiation, cells were stained with MF20 antibody recognizing all the myosin heavy chain and counterstained with Dapi (A). Fusion indexes were calculated by counting the number of nuclei in myotubes containing more than 2 nuclei

as the percentage of total number of nuclei (B). The transfections were performed 6 times for the unlipofected, 4 times for PMO-control, -PAS –DSE, and 2 times for PMO-CS1, CS2-, CS3. In each experiment, 1000 nuclei were counted. All data represent mean +/- Standard Deviation (SD).

Figure 6: Secondary structure predictions of *DUX4* mRNA

Mfold analysis was performed on the 3' end of *DUX4* (starting first nucleotide of exon 3 and ending 230 nucleotides downstream). The poly(A) signal and the cleavage region are boxed in red. The positions of the sequences recognized by the PMOs are in yellow for the PMOs inducing a strong down-regulation of *DUX4*, whereas the others are in blue. Examples of opened and closed RNA secondary structures are indicated.

TABLE LEGENDS

Table 1: Characteristics of the PMOs

PMO name	PMO sequence 5'-3'	Leash sequence 5'-3'	Length (bp)	%GC
PMO-PAS (-13 +12)	GGGCATTTTAATATATCTCTGAACT	gattgGATATATTAAAATGCCCgtgat	25	0.32
PMO-CS1 (-5 +32)	CTATAGGATCCACAGGGCATTTTAATATC	gttacCCCTGTGGATCCTATAGgtgat	29	0.38
PMO-CS2 (-1 +27)	GGATCCACAGGGAGGAGGCATTTTAATA	gattgTCCTCCCTGTGGATCCgtgat	28	0.46
PMO-CS3 (+2 +31)	TATAGGATCCACAGGGAGGAGGCATTTTAA	gaatgTCCCTGTGGATCCTATAgtgat	30	0.43
PMO-DSE (+32 +56)	CATCACACAAAAGATGCAAATCTTC	gattgGCATCTTTTGTGTGATGgtgat	25	0.36
PMO-Control	CCTCTTACCTCAGTTACAATTTATA	gattgTAACTGAGGTAAGAGGgtgat	25	0.32

N.A. : Non applicable

The locations, the PMO sequences and the leash sequences (uppercases indicate the complementary region between leash and PMO, lowercases indicates the free ends), the percentage of GC and the lenght are shown.

Table 2: Primers used in this study

	Targeted gene	Primer	Accession number	Sequence	Location	Size (bp)	qPCR efficiency (calculated from slope)
RT-oligonucleotides		Oligo_dT_3'RACE	N.A.	GCTGTCAACGATACGCTACGTAACGGCATGA CAGTGTTTTTTTTTTTTTTTTTTTTTTT	N.A	N.A	N.A
		Oligo_NVT	N.A.	GCGAGCTCCGCGGCCGCGTTTTTTTTTTVN	N.A.	N.A	N.A
PCR oligonucleotides	***DUX4-all***	DUX4-all_fw	ENSG00000260596	CCCAGGTACCAGCAGACC	Spanning Exon2-Exon3	164bp	N.A.
		DUX4-all_rev		TCCAGGAGATGTAACTCTAATCCA	Exon3		
	DUX4-3'UTR	DUX4-3'UTR_fw	HQ266760 (*DUX4-fl1*) and HQ266761 (*DUX4-fl2*)	AGGCGCAACCTCTCCTAGAAAC	Exon1	368bp and 504bp	N.A.
		DUX4-3'UTR_rev		TCCAGGAGATGTAACTCTAATCCA	Exon3		
qPCR oligonucleotides	***B2M***	B2M_fw	NM_004048.2	CTCTCTTTCTGGCCTGGAGG	Exon1	67bp	100%
		B2M_rev		TGCTGGATGACGTGAGTAAACC	Exon2		
	MBD3L2	MBD3L2_fw	NM_144614.3	CGTTCACCTCTTTTCCAAGC	Exon1	142bp	106%
		MBD3L2_rev		AGTCTCATGGGGAGAGCAGA	Exon2		
	TRIM 43	TRIM43_fw	NM_138800.1	ACCCATCACTGGACTGGTGT	Exon6	100bp	109%
		TRIM43_rev		CACATCCTCAAAGAGCCTGA	Exon7		
	ZSCAN4	ZSCAN4_962U20_fw	NM_152677.2	CTGGAGCAGTTTATGATTGG	Exon3	162bp	98%
		ZSCAN4_rev		AGCTTCCTGTCCCTGCATGT	Exon4		
3'RACE-PCR oligonucleotides		3RACE_3'_Primer_rev	N.A.	GCTGTCAACGATACGCTACGTAACG	N.A.	N.A	N.A
		3RACE_3'_Nested_rev	N.A.	CGCTACGTAACGGCATGACAGTG	N.A.	N.A	N.A
	DUX4	3RACE_Exon1_fw	ENSG00000260596	CTCTCCTAGAAACGGAGGCCCCG	Exon1	N.A	N.A
		3RACE_Exon1_Nested_fw		CTCGCTGGAAGCACCCCTCAGC	Exon1	N.A	N.A
		3RACE_3'_Exon3_fw	ENSG00000260596	CGCACCCCGGCTGACGTGCAAG	Exon3	N.A	N.A
		3RACE_3'_Exon3_Nested_fw		CGCTGGCCTCTCTGTGCCCTTG	Exon3	N.A	N.A

N.A. : Non applicable

Table 3: Prediction of the anti-DUX4 off target candidates

PMO name	Target name	E-value	% identity	No. of base overlap	Predicted homology with (+/-) strand	Coding/non-coding	Overall free binding energy (ΔGi)
PMO-PAS	*DUX4*	4,00E-05	100	25/25	-	Non-coding	-32.04
	IL1RAPL2	0.58	72	18/25	+	N.A	N.A.
	GYS2	2.3	68	17/25	-	Non-coding	-16.62
PMO-CS1	*C1ORF101*	0.91	72	21/29	+	N.A.	N.A.
	DUX4	3.6	59	17/29	-	Non-coding	-21.82
	PTPRT	3.6	59	17/29	-	Non-coding	-6.60
PMO-CS2	*DUX4*	2,00E-05	96	27/28	-	Non-coding	-38.02
	OTOF	0.82	75	21/28	+	N.A.	N.A.
	POR	0.82	64	18/28	+	N.A.	N.A.
PMO-CS3	*DUX4*	2,00E-05	97	29/30	-	Non-coding	-37.93
	OTOF	0.99	70	21/30	+	N.A.	N.A.
	POR	0.99	60	18/30	+	N.A.	N.A.
PMO-DSE	*DUX4*	4,00E-05	100	25/25	-	Non-coding	-27.41
	TCRA/TC	0.58	72	18/25	+	N.A.	N.A.
	KCNJ6	2.3	68	17/25	+	N.A.	N.A.

N.A. : Non applicable

Each PMO sequence was run thought the BLAST software, optimised for short input sequences and limited to human and nt/nr database. Overall binding energy was calculated only for the predicted targets that show sequence homology with the PMO on their negative strand (-). The units of ΔGi are expressed in kcal/mol. Abbreviations: *IL1RAPL2*, interleukin 1 receptor accessory protein-like 2; *GYS2*, glycogen synthase 2; *C1ORF101*, chromosome 1 open reading frame 101; *PTPRT*, protein tyrosine phosphatase receptor type T; OTOF, otoferlin; *POR*, P450 cytochrome oxidoreductase; *TCRA/TCRD*, T cell receptor alpha delta locus; *KCNJ6*, potassium channel inwardly rectifying subfamily J member.

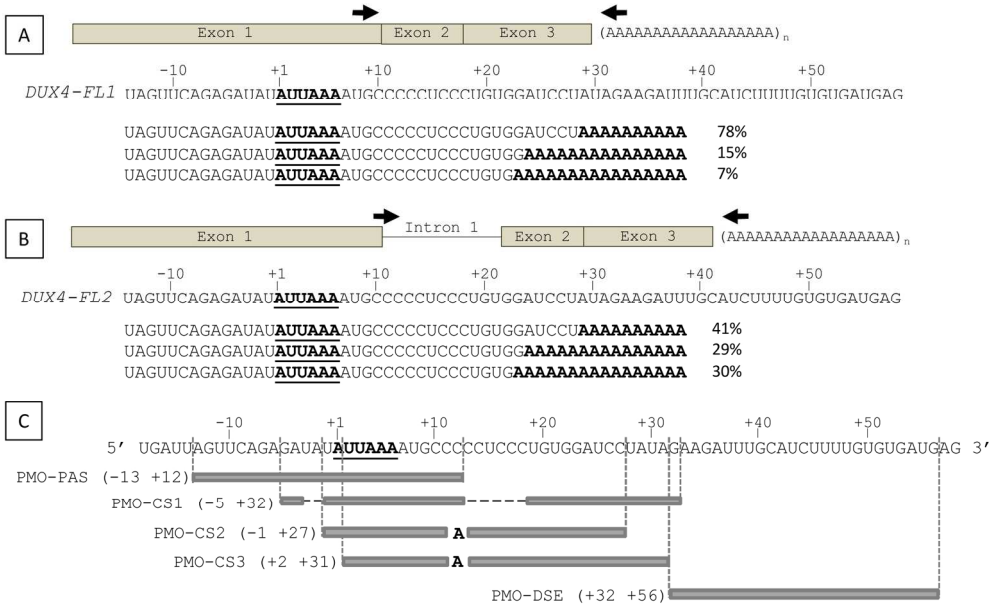

Figure 1: 3'end key elements of DUX4 mRNA and PMO design.
A and B: To determine the cleavage sites of DUX4 mRNA, a RT using an oligo dT adapter primer was realized on total mRNAs isolated from FSHD myotubes at day 4 of differentiation. The 3'RACE-PCR was performed using forward primer matching exon 1 and reverse primer recognizing the adapter. The PCR products were cloned into a TOPO-TA plasmid and 27 and 17 clones were sequenced for DUX4-FL1 (A) and –FL2 (B) respectively. The frequencies of the cleavage site usages are indicated. Arrows indicate the location of the primers used. The poly(A) site is bolded and underlined and the poly(A) tail is in bold.
C: Sequences recognized by the different PMOs targeting DUX4. The position +1 is defined as the first base of the poly(A) site. The sequences recognized by the PMOs are indicated as well as their position on the mRNA. Deletions are represented by hyphen (-). Nucleotidic substitutions are indicated.
180x108mm (300 x 300 DPI)

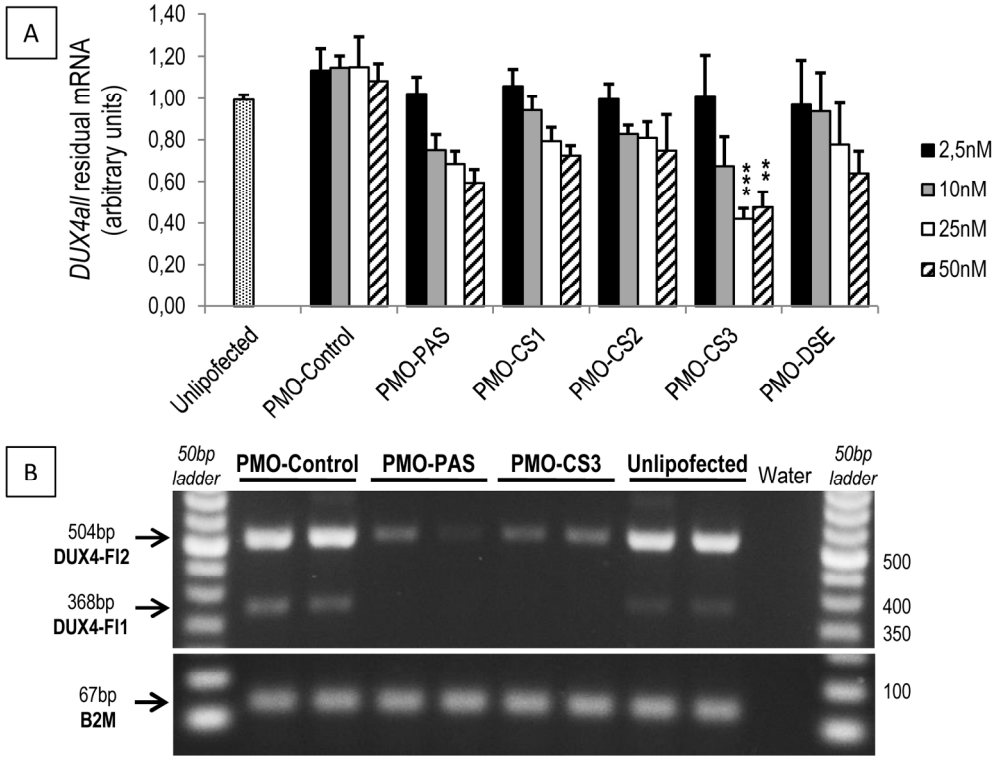

Figure 2: DUX4 expression in the presence of the PMOs
Immortalized FSHD myotubes were transfected with PMOs in a dose dependent manner. (A) The percentage of residual DUX4-all mRNA was measured by semi quantitative PCR using ImageJ software on gel scans. Independent transfections for PMO-control, -PAS, -CS1, -CS2, CS3, and -DSE (n≥6) were performed. Values are compared to unlipofected conditions. All data represent mean +/- Standard Error of Mean (SEM). A multiparametric analysis of variance and a Newman–Keuls post hoc test were performed (*p<0.05; **p<0.01; ***p<0.001). (B): Representative RT-PCR analysis using DUX4-3'UTR primers in the presence of PMO-control, PAS, and -CS3 at 50 nM. As a negative control, a PMO targeting a human β-globin mutation that causes β-thalassemia was be used. B2M was used as the reference (housekeeping) gene.
153x117mm (300 x 300 DPI)

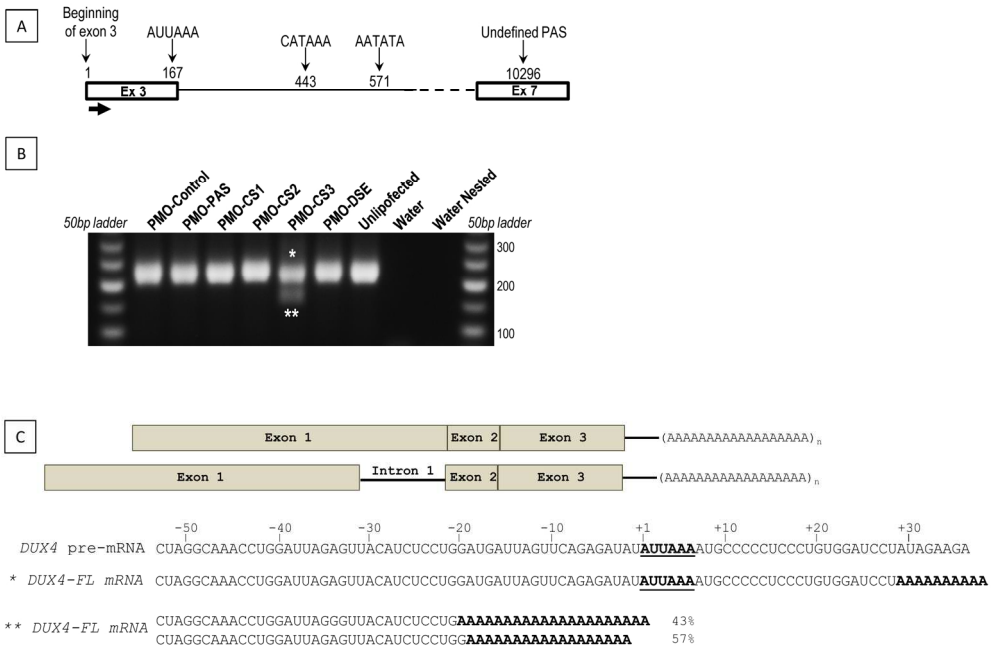

Figure 3: PMO-CS3 induces a switch in cleavage site usage.
A redirection of poly(A) usage was investigated in the presence of the different PMOs. (A) In silico analyses and literature (18) reveal the presence of alternative polyadenylation site in the subtelomeric region of chromosome 4. (B) 3'RACE nested PCR using forward primers located in exon 3 shows a switch in cleavage site only in the presence of PMO-CS3. The bands with (**) or without (*) a redirection of the cleavage site are indicated. (C) Sequence of the most abundant mRNA carrying the redirected cleavage site (DUX4 pre-mRNA). The sequence of poly(A) site is underlined and bolded. The poly(A) tail is in bold. The frequencies of each variant showing alternative cleavage site usage are indicated (14 analyzed sequences).
180x116mm (300 x 300 DPI)

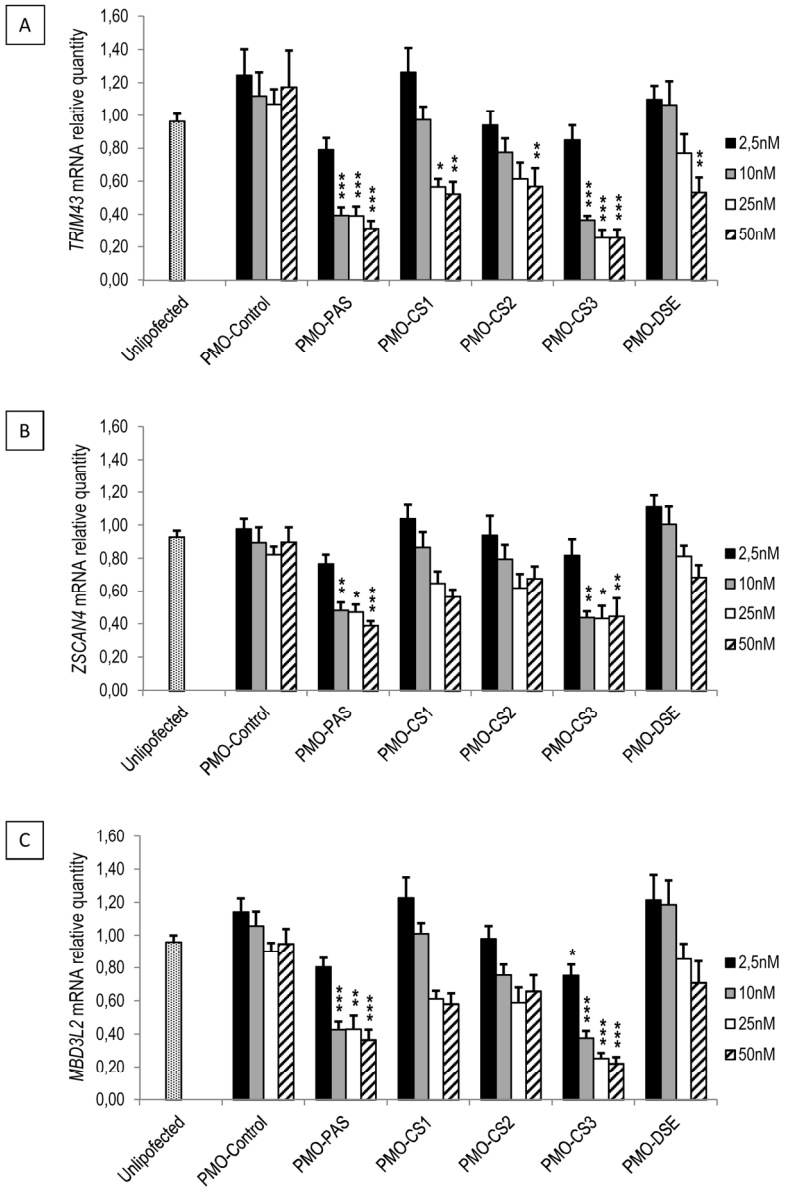

Figure 4: Expression of the genes downstream of DUX4 in presence of the PMOs
Expression levels of TRIM43 (A), ZSCAN4 (B) and MBD3L2 (C) were measured by RT-qPCR in FSHD myotubes (4 days of differentiation) in the presence of the PMOs at different concentrations and compared to the PMO control at the same concentration. Values are compared to unlipofected conditions. B2M was used as a normalizer. Data represent mean +/- standard error of mean from independent transfections for PMO-control, -PAS, -CS1, -CS2, CS3, and -DSE (n≥6). A multiparametric analysis of variance and a Newman–Keuls post hoc test were performed (*p<0.05; **p<0.01; ***p<0.001).
135x199mm (300 x 300 DPI)

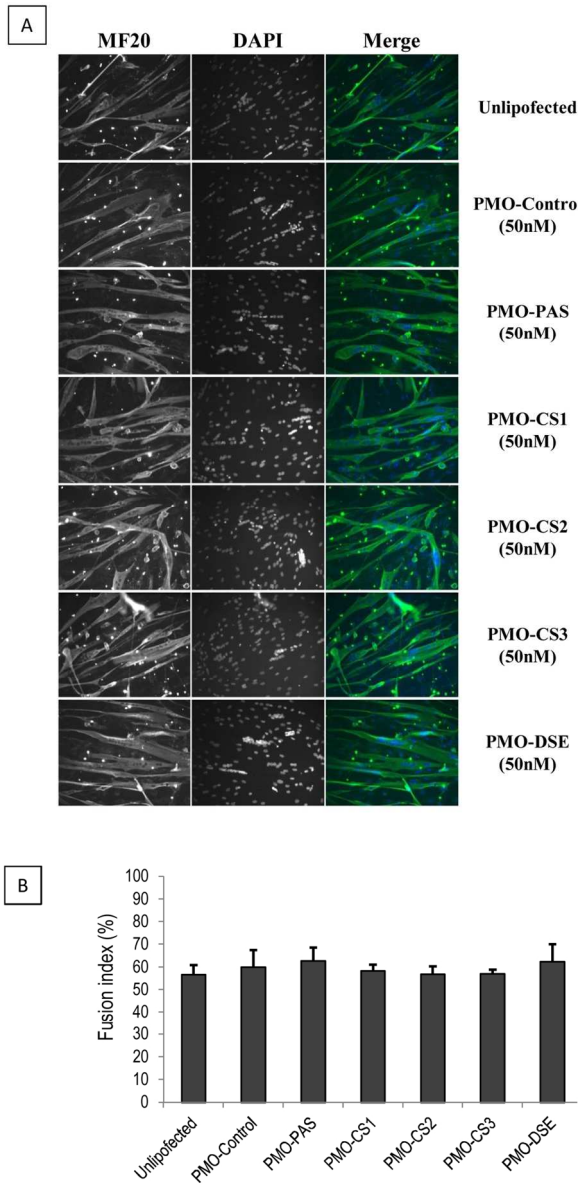

Figure 5: Fusion index of immortalized FSHD myotubes in the presence of the PMOs
Immortalized FSHD myotubes were transfected at day 2 of differentiation with the different PMOs at 50 nM. At day 4 of differentiation, cells were stained with MF20 antibody recognizing all the myosin heavy chain and counterstained with Dapi (A). Fusion indexes were calculated by counting the number of nuclei in myotubes containing more than 2 nuclei as the percentage of total number of nuclei (B). The transfections were performed 6 times for the unlipofected, 4 times for PMO-control, -PAS –DSE, and 2 times for PMO-CS1, CS2-, CS3. In each experiment, 1000 nuclei were counted. All data represent mean +/- Standard Deviation (SD).
86x178mm (300 x 300 DPI)

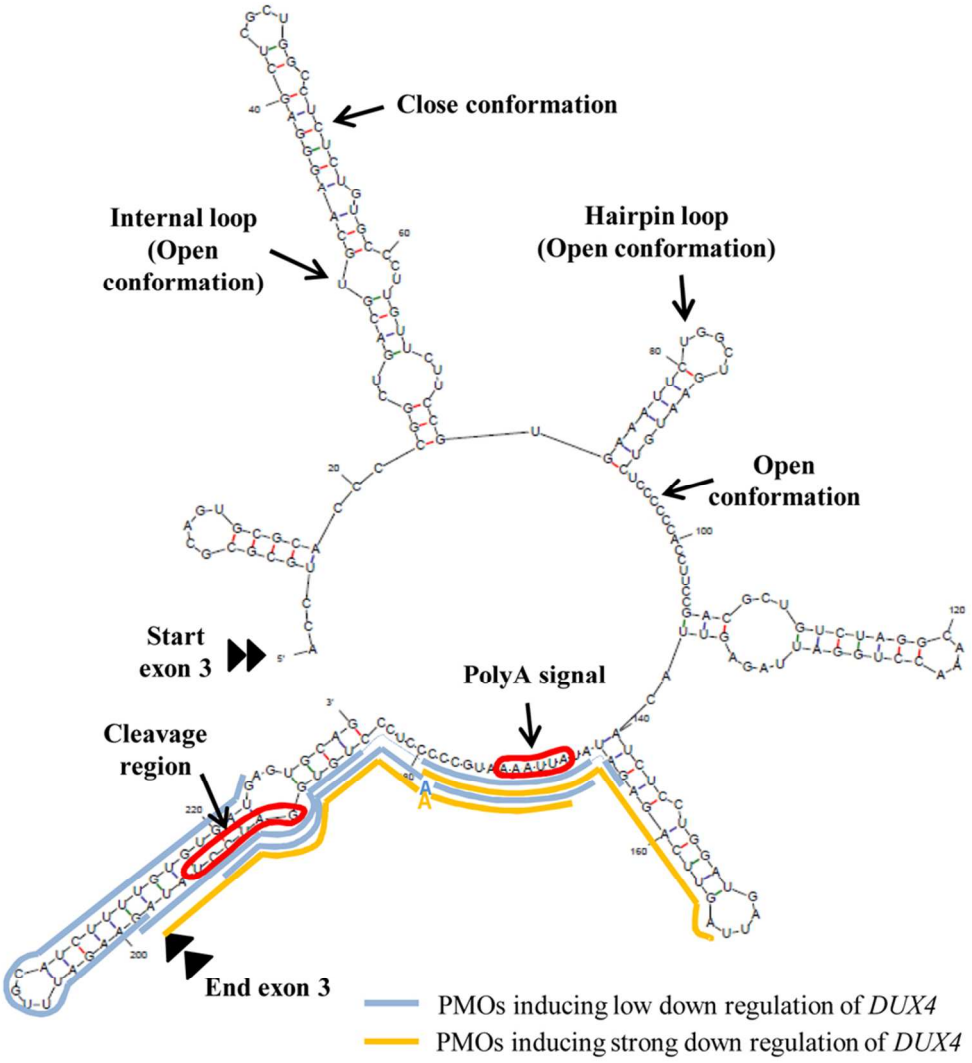

Figure 6: Secondary structure predictions of DUX4 mRNA
Mfold analysis was performed on the 3' end of DUX4 (starting first nucleotide of exon 3 and ending 230 nucleotides downstream). The poly(A) signal and the cleavage region are boxed in red. The positions of the sequences recognized by the PMOs are in yellow for the PMOs inducing a strong down-regulation of DUX4, whereas the others are in blue. Examples of opened and closed RNA secondary structures are indicated.
86x93mm (300 x 300 DPI)